CHAPTER-2

LITERATURE SURVEY

Bubble columns are gas-contacting devices in which gas is sparged into liquid. The mixing is induced due to bubbles rising through the liquid. The columns may be operated in batch mode or continuous mode with reference to the role of the liquid. If the liquid is also flowing then the bubble column is said to be operated in continuous mode or else it is in the batch mode of operation.

Bubbles columns are used for reactions in which one of the reactant is present in the gas phase e.g. hydrogenation, chlorination, oxygenation etc. These also find use in biochemical operations, wastewater treatment etc.

To understand the performance of bubble columns it is necessary to understand the degree of mixing, which determines the heat and mass transfer coefficients. Since the mixing is induced mixing due to movement of bubbles, the bubble behaviour such as bubble velocity, bubble size and bubble shape are important parameters.

The observed rate of reaction between the reactants present in liquid and gas phases depends upon the interfacial area and mass-transfer coefficient. The gas-liquid interfacial area depends upon the bubble behaviour. To some extent the mass-transfer coefficient also depends upon the bubble behaviour,

A discussion on various aspects of bubble behaviour and measurement of gas-liquid interfacial area, based on the available literature is presented in the following section.

2.1 Flow Regime:

Depending on the superficial gas velocity three types of main flow regimes, as shown in Fig. 2.1, have been observed in bubble columns [Shah et al. (1982)]. Though, few more less popular flow regimes have been reported in literature [Kumar et al. (1976)].

2.1.1 Homogeneous Flow or Bubbly Flow Regime:

At very low superficial gas velocity there are few bubbles only. The bubbles are of almost of uniform size. Kumar et al. (1976) subdivided this into regimes. When the bubbles moved freely as individuals it was named as dispersed flow regime. When the bubbles moved as swarm of bubbles it was named as fluidized regime. The bubble size depends on the specification of the sparger, where the bubbles are found. These bubbles rise vertically undisturbed [Zahradnik and Kastanek (1975)]. Due to the absence of bubble coalescence and bubble breakup the size of the bubbles remain unchanged until they are disengaged from the top. The scope of liquid circulation is more due to small size of bubbles. The liquid phase turbulence is not isotropic [Kantarci et al. (2005)].

Schumpe and Deckwer (1982) observed that flow regime depends upon the type of the sparger also. For sintered plate homogenous flow regime was observed but for perforated plate this kind of flow was not observed at small values of superficial gas velocity.

2.1.2 Heterogeneous Flow Regime:

When the superficial gas velocity is increased, the number of bubbles in the column increases. The bubbles are closed enough to interact at initial bubble collisions. The collapsed bubbles move at increased velocity causing a liquid circulation. These liquid circulations have been modelled as liquid circulation cell [Joshi et al. (1979)].

Whenever liquid turbulence is high, the large bubbles may break into small bubbles [Hinze (1955)]. Bubbles are of various sizes with wide distribution. The residence time of bubbles is not uniform. Liquid turbulence is generally assumed to be isotropic. The transition from homogeneous to heterogeneous flow regime is at the range of 0.05-0.1 m/s superficial gas velocity. For perforated plate even at small values of superficial gas velocity bubbles of various sizes were observed due to bubble coalescence and this type flow was observed.

Kantarci et al. (2005) observed existence of radial gas hold-up profile. A portion of the gas is transported through the bed in the form of fast moving bubbles. This fraction increases with increasing gas velocity. The mass-transfer coefficient is lower in heterogeneous regime than that in homogeneous flow regime.

2.1.3 Slug Flow Regime:

In case of small diameter column (< 0.15m) as the gas velocity increased further, the bubble size increased due to bubble collisions. So that the bubble diameter becomes equals to the column diameter. The liquid turbulence is not sufficient to break the bubble of this size. Therefore, the some of the bubbles flow in terms of slug. Schumpe and Deckwer (1982) studied transition of flow regime to slug flow regime for various concentrations of CMC solution in a 0.15 m diameter column. Bukur and Patel (1989) also observed that in a small column the homogeneous flow and slug flow regimes were present. In large column homogeneous flow and churn turbulent flow were observed.

In addition to this sometimes the large bubbles move in the form of spiral. This has been named as Vortical-Spiral Flow Regime [Chen et al. (1994)] who considered this to be a subdivision of heterogeneous flow regime.

Sometimes a cellular foam like structure in the bed has been observed. It is not due to any foaming agent but is due to hydrodynamic conditions in the bed [Zahradnik and Kastanek (1997)] called this as Foam Regime. Kumar et al. (1976) have mentioned two flow regimes namely froth regime and foam regime. The flow regime was based on the values of gas holdup.

Kazakis et al. (2007) defined pseudo- homogeneous flow regime as a subdivision of homogeneous flow regime. The bubbles are generated at the sparger. The gas holdup increases linearly with superficial gas velocity but no radial uniform distribution of bubbles is observed.

Industrial bubble columns operates in the range of gas velocity of 0.01 to 0.5 m/s. since the column diameter is large slug flow regime is absent in industrial bubble columns. The flow regimes depend on type of gas sparger used, operating gas velocity, fluid properties and column diameter. These parameters also influence bubble size, its distribution, gas holdup, bubble velocity and transfer coefficients.

Transition of regime from Homogeneous to Heterogeneous is important as the hydrodynamic behavior of the system changes significantly. The gas velocity for transition regime depends on sparger design, physical properties of the system and column dimensions [Thorat and Joshi (2004)] though exact correlation is not available.

2.2 Gas Holdup:

Gas holdup, ε, in bubble columns have been studied extensively and have been reviewed from time to time. It is defined as ratio of volume fraction of gas phase in the form of gas bubbles to the total volume of gas-liquid dispersion. It is considered to be an important hydrodynamic parameter which affects even transport properties in bubble columns [Verma (1989), Verma and Rai (2003)].

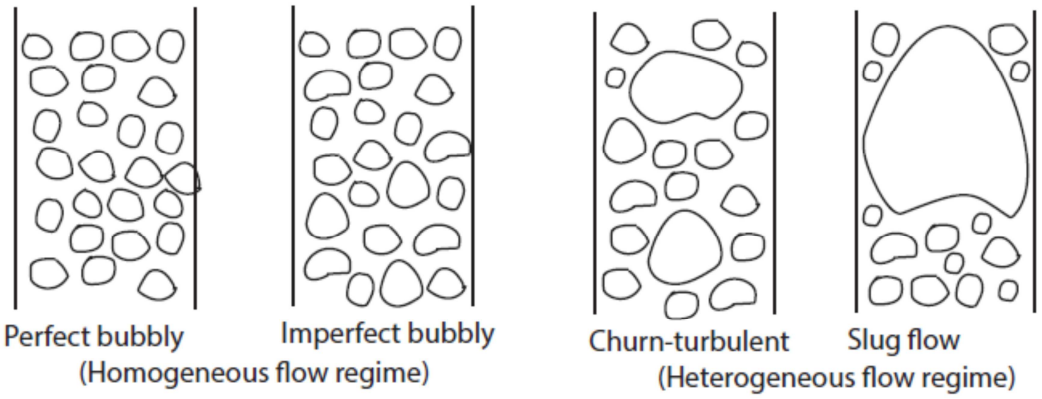

Figure 2.1: Flow regimes in bubble columns [adopted from Shah et al. (1982)].

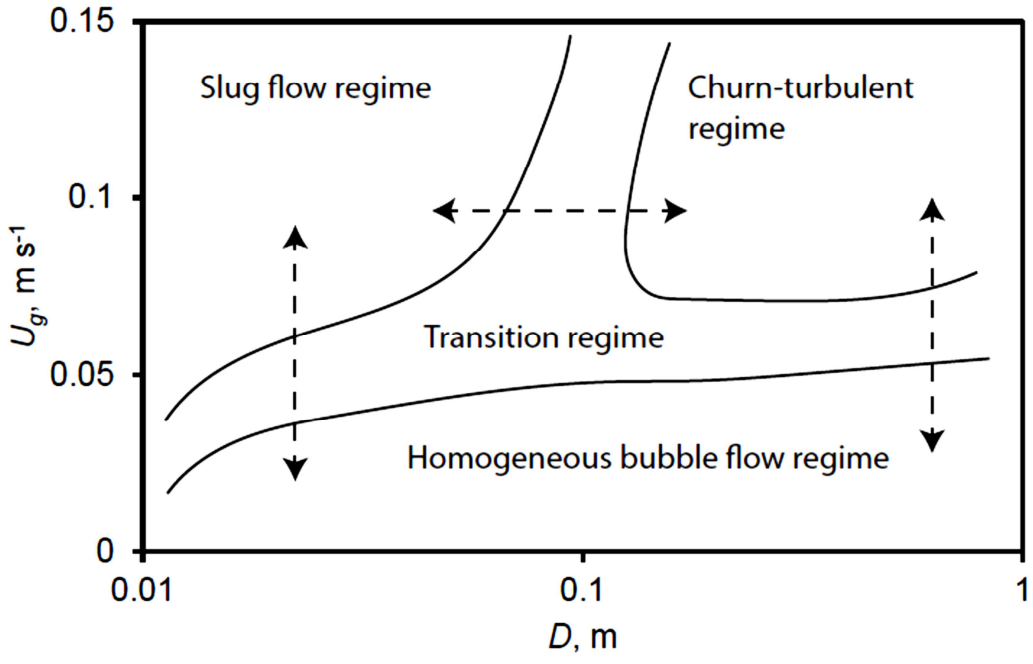

Figure 2.2: Flow regime map [adopted from Shah et al. (1982)].

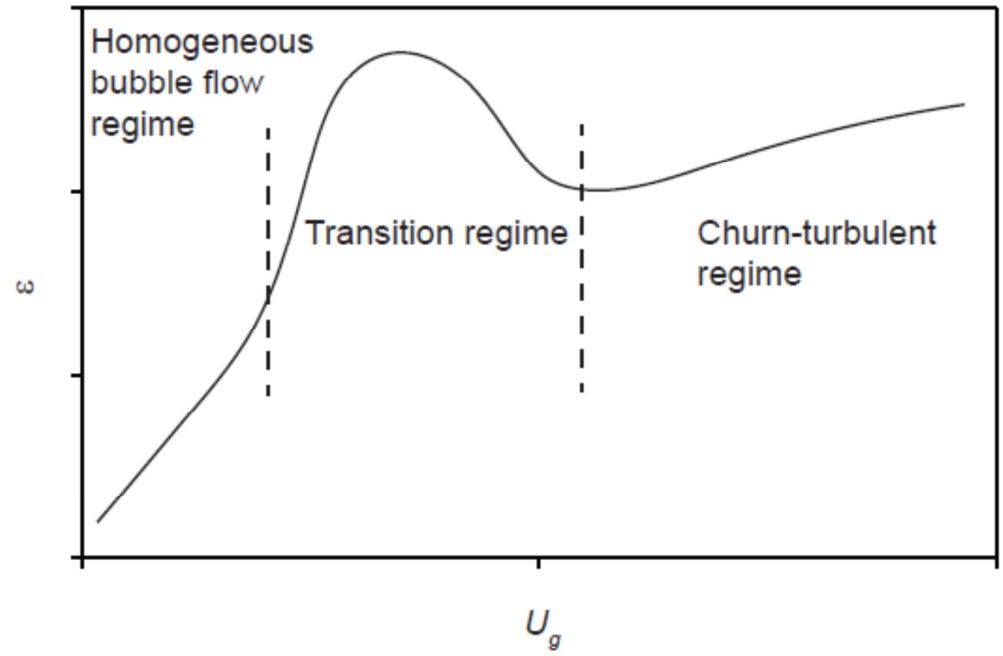

Figure 2.3: Dependence of flow regimes on gas velocity [adopted from Zahradnik et al. (1982)].

Various correlations for gas holdup proposed in the literature are presented in Table 2.1. Correlations by Bach and Pilhofer (1978), Akita and Yoshida (1973), Hikita et al. (1980) and Koide et al. (1984), expresses gas holdup in terms of *Bo*, *Fr*. *Ga* and *Re*, though exponents of these are different in each of these correlations because each correlations have different functions of Ɛ. Akita and Yoshida (1973) and Koide et al. (1984) used $\varepsilon/(1-\varepsilon)^4$, Bach and Pilhofer (1978) used $\varepsilon/(1-\varepsilon)$ and Hilkita et al. (1980) used ε to correlate their data. Correlation by Hikita et al. (1980) used density

ratio and viscosity ratio of gas and liquid phases respectively in addition to all four dimensionless numbers.

Effect of number of holes, their placement on perforated plate sparger on gas holdup was revealed that the number of holes affected gas holdup strongly at high superficial gas velocity, the effect of viscosity had significant effect only at low gas velocities [Guy et al (1986)]. The correlation for gas holdup was in terms of dimensionless numbers, though, Ga_o and Fr_o were based on orifice dimensions in place of column diameter. The equivalent diameter, D_E, was same as column diameter, D, in case of symmetrical sparger. When holes were placed on one side of the distributor plate, the value of D_E was taken as ratiof of area of zone on plate having holes to perimeter of the plate.

Earler correlations considered column diameter, D, as the only geometrical parameter. Different type of sparger is may affect the gas holdup and other properties. In a study, gas holdup was measured in four bubble columns, three with perforated plate (PP) sparger having holes of different sizes (421×0.005 m, 73×0.001, 19×0.002 m) and one with sintered plate (SP) sparger [Shumpe and Deckwer (1982)]. Water and CMC solution (as non-Newtonian fluid) were employed. No effect of viscosity in case of slug flow was observed. However, different correlations for each bubble column and for homogeneous and slug flow regimes were proposed. No single correlation could be obtained. The study clearly indicated the importance of sparger in affecting the gas holdup.

Table 2.1: Correlations for gas holdup in bubble columns (PP=Perforated plate, SN=Single nozzle, SP=Sintered plate), PoP= Porous Plate, RGS= Radial Gas Sparger). The dimensionless numbers used are Eotvos number or Bond's Number, $Eo = Bo = gD^2\rho_l/\sigma_l$; Morton number, $Mo = \mu_l^4 g/\rho_l\sigma^3$; Reynold's number, $\mathrm{Re} = DU_g\rho_l/\mu_l$; Froude number, $Fr = U_g/\sqrt{gD}$; Galileo Number, $Ga = gD^3\rho_l^2/\mu_l^2$; Weber number, $We = \rho_g U_g^2 D^4/\left(n_o^2 d_o^3\sigma\right)$; Archimedes Number, *Ar*, is same as *Ga*

Investigator	Correlation	System	Column
Hughmark (1967)	$\varepsilon = \left[1/\left\{2+\left(0.35/U_g\right)\left[\rho_l\left(\sigma_l/0.072\right)\right]^{1/3}\right\}\right]$	Air/water, Versol, Glycerol, Na_2CO_3 soln., $ZnCl_2$ soln.	D=0.0254, 0.0508, 0.1524, 0.3048m
Akita and Yoshida (1973)	$\varepsilon/(1-\varepsilon)^4 = 0.20Bo^{1/8}Ga^{1/12}Fr$	Air, oxygen, helium/water, glycol, glycerol, methanol, 0.15M Sodium sulphite solution	D=0.152, 0.301, 0.6 m SN(d_o=0.005 m)
Kumar et. al. (1976)	$\varepsilon = 0.728U_g^* - 0.485U_g^{*2} + 0.0975U_g^{*3}$ Where $U_g^* = U_g\left[\rho_l^2/\left\{\left(\rho_l-\rho_g\right)\sigma\right\}\right]^{1/4}$	Air, Water, Glycerol (40%),, Kerosene CO_2, Aqueous NaOH (2M)	D=0.05, 0.075, 0.1 m SN (d_o=0.00087, 0.00153, 0.00196, 0.00265, 0.00309 m, n_o=1)
Bach and Pilhofer (1978)	$\varepsilon/\left(1-\varepsilon\right) = 0.115\left(\mathrm{Re}\,Fr'\right)^{0.23}$; *Fr'=Fr*^{2}	Air, water, butan-1,3-diol, ethylene glycol, tetrabromoethane, n-octanol	D = 0.1 m PP(d_o= 0.0005 m)

Hikita et. al. (1980)	$\varepsilon = 0.672\left(\frac{U_g \mu_l}{\sigma}\right)^{0.578}\left(\frac{\mu_l^4 g}{\rho_l \sigma^3}\right)^{-0.131}\left(\rho_g/\rho_l\right)^{0.062}\left(\mu_g/\mu_l\right)^{0.107}$	Air, H_2, CO_2, CH_4, C_3H_8, N_2, water, sucrose, methaol, n-aniline, i-butanol, NaCl, Na_2SO_4, $CaCl_2$, $MgCl_2$, $AlCl_3$, KCl, K_2SO_4, K_3PO4, KNO_3	D=0.1 m SN (d_o=0.011 m, n_o=1)
Kara et. al. (1982)	$\varepsilon = \mathrm{Re}/(1521.23 + 3.75\,\mathrm{Re})$	Air, water, coal, dried mineral ash	D=0.152 m
Schumpe and Deckwer (1982)	$\varepsilon = 0.0908U_g^{0.85}$ $\varepsilon = 0.0258U_g^{0.876}$ $\varepsilon = 0.0322U_g^{0.674}$ $\varepsilon = 0.404U_g^{0.627}$	Air, CMC (0-2%) Na_2SO_4 (0.8mol/l)	D=0.102, 0.14 m SP (d_o=0.00015, 0.0002 m) PP [(d_o=0.0005 m, n_o=421), (d_o=0.001 m, n_o=73), d_o=0.002 m, d_o=19)]
Deckwer et al. (1982)	$\varepsilon = 0.0265U_g^{0.82}$; for slug flow refime at U_g>0.02 ms^{-1}	Air/Water,CMC solution	D=0.14 m; PP(n_o=73,d_o=0.001m; n_o=19,d_o=0.002m),SP(d_o=0.0002m) ; Rubber plate with 1000 pricks
Sada et. al. (1984)	$\varepsilon/(1-\varepsilon)^4 = 0.32Bo^{0.121}Ga^{0.086}(\rho_g/\rho_l)^{0.068}Fr$	N_2, He, CO_2, O_2, glycerol, Na_2SO_4, mixture of LiCl(58 mol%)-KCl(42 mol%) with molten $NaNO_3$	D=0.073 m SN(d_o=0.0015, 0.0027, 0.0057m)
Reilly et. al. (1986)	$\varepsilon = 296U_g^{0.44}\rho_l^{-0.98}\sigma^{-0.16}\rho_g^{0.19} + 0.009$	Air, He, Ar, water, varsol, trichloroethylene, glassbeads	D = 0.3 m PP (d_o=0.0015 m, n_o=293; d_o=0.0134 m, n_o=6), SN(d_o=0.0254 m)

Guy et. al. (1986)	$\varepsilon = 0.386 n_o Ga_o^{0.025} Fr_o^{0.84} (d_o / D_E)^{2.075}$	Air, water, glycerol, CMC, polyacrylamide Separan	D=0.254 m PP [(d_o=0.001 m, n_o=60), (d_o=0.001 m, n_o=61), (d_o=0.001 m, d_o=33)]
Renjun et. al. (1988)	$\varepsilon = 0.17283 Mo^{-0.1544} \left(P + P_S\right) / P^{1.6105} \left(U_g \mu_l / \sigma\right)^{0.5897}$	Air, water, alcohol, 5% NaCl	D=0.1 m SN(d_o=0.01 m)
Bukur and Patel (1989)	For pure liquids same as Bach and Pilhofer (1978) $\varepsilon = U_g^{K_1}(1+C_N)^{0.167} \Big/ \left(K_2 + \left\{K_3 / U_g^{K_4}\right\}\left\{\rho_l \sigma / 0.072\right\}^{K_5}\right)$; ($C_N$ is carbon number, for butanol solution) $\varepsilon / \left(1-\varepsilon\right)^4 = 0.032 Bo^{-0.056} Ga^{0.31} Fr^{1.2} We^{0.25}$; (for PP and SN distributors, solutions) $\varepsilon = 1.42 U_g \mu_l^{-0.27}$; (for SP distributor, solutions)	N_2, water, n-butanol, CMC	[D=0.05 m; SN(d_o=0.001, 0.00185m), SP(d_o=40μm)], D=0.23 m; PP(n_o=19, d_o=0.001,0.00185m)
Kawase and Moo-Young (1989)	$\varepsilon = 1.07(1-a)^{1/3} Fr^{1/3}; a = \tau_0 / (R/2)$	Air, Carbopol	[D=0.23 m; PP(n_o=20, d_o=0.001m)], [D=0.76 m; RGS (D_S=0.35 m, H_S=1.95 m, n_o=128, d_o=0.0018-0.0023m)]
Mok et. al. (1990)	$\varepsilon = 0.107 \times 10^{-4} \mathrm{Re}_g^{1.09} Ga^{0.096} (d_o / D)^{-0.19}$	Oil free Air, Water, CMC (0.05, 0.075, 0.1, 0.15, 0.2, 0.3 wt%)	D=0.14 m PP (d_o=0.0003 m, n_o=51)
Ryu et. al. (1993)	$\varepsilon = 12.00 Fr^{1.220} Ga_{eff}^{0.025}$ in homogeneous flow $\varepsilon = 0.922 Fr^{-0.222} Ga_{eff}^{0.365}$ in churn-turbulent flow	Air, CMC (0.7 wt. %)	D=0.115 m RGS (D_S=0.038 m, H_S=0.15 m, d_o=5 μm)
Choi et. al. (1996)	$\varepsilon = 1.034 U_g^{0.704}$	Air, water, glass beads	0.456 m* 0.153m PP (d_o=0.002 m, n_o=30, 15)

Degaleesan et. al. (1997)	$\varepsilon = 0.07U_g^{0.474-0.00626D}$, for D>0.1 m	Synthesis gas, Oil, Mn particles	D = 0.46 m
Godbole et al. (1982)	$\varepsilon = 0.319U_g^{0.476}\mu_l^{-0.058}$	Air, water, glycerine, CMC	D=0.305 m PP (d_o=0.00166 m, n_o=749)
Pohorecki et. al. (2001)	$\varepsilon = 0.383U_g^{0.65}\sigma^{-0.52}$	N_2, Cyclohexane	D=0.304 m (d_o=0.001-0.005 m, n_o=1-27)
Jordan and Schumpe (2001)	$\frac{\varepsilon}{(1-\varepsilon)} = K_1 Bo^{0.16} Ga^{0.04} Fr^{0.70}\left[1+27.0Fr^{0.52}\left(\frac{\rho_g}{\rho_l}\right)^{0.58}\right]$	N_2, He, Ethanol(96%),1-Butanol, Toluene, Decalin	D=0.1 m, PP (d_o=0.0043 m, n_o=1, d_o=0.001 m, n_o=1, d_o=0.001 m, n_o=19)
Syeda et. al. (2002)	$\varepsilon = 1.334\left[(We/2)^{1/2}\right]^{0.032}\left(U_g\mu_l/\sigma\right)^{0.578}\left(\mu_l^4 g/\rho_l\sigma^3\right)^{-0.131}$ $\left(\rho_g/\rho_l\right)^{0.062}\left(\mu_g/\mu_l\right)^{0.107}$ In case of binary mixtures $(We_1/2)^{1/2}$ is replaced by $x(We_1/2)^{1/2}+(crk^2/\sigma)+(1-x)(We_2/2)^{1/2}$ Where $c=(2/CRT)\theta(x)(d\sigma/dx)$, $\theta(x)=x(1-x)/(1-x-xV_1/V_2)$ and $k=(12\pi\sigma/Ar)^{1/3}$; C=molar density of mixture	Air, water, methanol, 2-propanol, ethylene glycol	D=0.09 m PP (d_o=0.005 m, n_o=25, d_o=0.003 m, n_o=75)
Anabtawi et. al. (2003)	$\varepsilon = 0.362U_g^{0.6}\mu_l^{-0.24}H^{-0.38}$; For cylindrical column $\varepsilon = 0.549U_g^{0.81}\mu_l^{-0.15}H^{-0.22}$; For bi-directional column	Air, light oil, machine oil, engine oil	0.0195m×0.22m, D = 0.074m, SN(d_o=0.01 m)
Urseanu et. al. (2003)	$\varepsilon = 0.21U_g^{0.58}D^{-0.18}\mu_l^{-0.12}\rho_g^{\left[0.3\exp(-9\mu_l)\right]}$	N_2, tellus oil, glucose	[D = 0.15m, PP (d_o=0.0005 m, n_o=200)] [D = 0.23m, PP (d_o=0.0005 m, n_o=200), RGS (n_o=16, d_o=0.0015

			m)]
Fransolet et. al. (2005)	$\varepsilon = 0.26 U_g^{0.54} \mu_{eff}^{-0.147}$	Air, water, xanthan	D = 0.24 m PP (d_o=0.001 m, n_o=203)
Mouza et. al. (2005)	$\varepsilon = 0.001\left[Fr'^{0.5} Ar^{0.1} Eo^{2.2} \left(d_s/D\right)\right]^{2/3}$	Air, water, butanol, glycerin	0.1 m×0.1 m PoP (20, 40 µm)
Behkish et. al. (2006)	$\varepsilon = 0.00494\left(\rho_l^{0.415}\rho_g^{0.177}/\mu_l^{0.174}\sigma^{0.27}\right)U_g^{0.553}\left[P/(P-P_v)\right]^{0.203}\left[D/(D+1)\right]^{-0.117}$ $\left(K_d \times n_o d_o^{\alpha}\right)^{0.053}\exp\left[-2.231C_S - 0.157\rho_P d_{32} - 0.242X_W\right]$		Data available in literature is used for correlations
Kazakis et. al. (2007)	$\varepsilon = 0.2\left[Fr^{0.8} Ar^{0.2} Eo^{1.6} \left(d_s/D\right)^{0.9} \left(d_o/d_s\right)^{0.03}\right]^{2/5}$	Air, water, n-butanol, glycerin, kerosene	D = 0.09 m PoP (40, 100 µm)
Thaker and Rao (2007)	$\varepsilon = 1.4 U_g^{0.83} \left(H/D\right)^{0.09}$	Pure CO_2, distilled water, Aqueous NaOH solution (1N)	D=0.14 m PP (d_o=0.001 m, n_o=24)
Jin et. al. (2007)	$\varepsilon = 1.042 U_g^{0.523} \left(H/D\right)^{-0.096}$	Air, water	D = 0.16 m PP (d_o=0.001 m, n_o=55)
Anastasiou et. al. (2010)	$\varepsilon = 0.14\left[Fr^{1.0} Ar^{0.15} Eo^{1.85} \left(d_s/D\right)^{0.2} \left(d_o/d_s\right)^{-0.3}\right]^{0.37}$; For ionic surfactants $\varepsilon = 0.0034\left[Fr^{0.6} Ar^{0.15} Eo^{1.85} \left(d_s/D\right)^{0.2} \left(d_o/d_s\right)^{-0.3}\right]^{0.52}$ For non-ionic surfactans	Air, TritonX-100, SDS, CTAB	D = 0.09 m PoP (40 µm)
Maceiras et. al. (2010)	$\varepsilon = 1.83\times10^{-9} Fr^{0.45} Ar^{0.62} Eo^{0.7} \left(d_{32}/D\right)^{-1.3}$	CO_2, diethanolamine	0.06x0.06m column; PoP (d_o=0.004 m)
Asgharpour et. al. (2010)	$\varepsilon = 0.55 d_{32}^{0.101} U_g^{0.925} \sigma^{-0.54}$	Air, Distilled water (n-decane, n-tridecane, n-	D=0.095 m PP (d_o=0.0003 m, n_o=26)

		hexadecane used as impurities)	
Cachaza et. al. (2011)	$\varepsilon = 1.83U_g^{0.97}\left(C/C_t\right)^{0.08}$; C=conc. of surfactant, C_t=conc. of surfactant at flow transition. In absence of surfactant C/C_t=1	Air, water, $CaCl_2$, NaCl, KCl, EtOH, POH, IBOH	0.2 m×0.04 m PP (d_o=0.001 m)
Anastasiou et. al. (2013)	$\varepsilon = 2.2\left[Fr^{1.07}Ar^{0.84}Eo^{0.19}\left(d_o/D\right)^{1.16}\left(d_o/d_s\right)^{2.86}\right]^{0.264}$	Air, glycerin, xanthan	D = 0.09 m PoP (40 μm)
Jin et. al. (2013)	$\varepsilon = 0.2064U_g^{0.787}\left(n_o d_o^2/D^2\right)^{-0.674} d_o^{-0.178}\left(\theta\pi/180\right)^{-0.203}$	Air, water	D = 0.3 m PP(d_o=0.002 m, n_o=98)
Sal et. al. (2013)	$\varepsilon = 0.2278\left(Fr^{0.7767}Ar^{0.3649}\left(d_o/D\right)^{0.4780}\right)\Big/\left(Eo^{0.3916}We^{0.2402}\right)$	Air, water	D = 0.33 m PP(d_o=0.001 m, n_o=817; d_o=0.002 m, n_o=217; d_o=0.003 m, n_o=91)
Kojima et. al. (1997)	$\varepsilon = 1.18U_g^{0.679}(\sigma/0.076)^{-0.546}\times\exp[K_1(\rho_l Q^2 d_o^{-3}\sigma^{-1})(P/P_o)^{K_2}]$ The constants K_1 and K_2 depends upon enzyme conc. Q =volumetric flow rate of gas	N_2 - O_2, water, NaH_2PO_4-citric acid solution, glucose oxidase	D = 0.045 m SN(d_o=0.00138, 0.0021, 0.0029, 0.00403 m)

2.2.1 Effect of Sparger Geometry on Gas Holdup:

It may be argued since the initial value of bubble diameter produced at the sparger depends upon the nozzle diameter of the sparger. Later correlations included nozzle diameter also. However, there are several types of sparger which with same nozzle diameter may produce different gas holdup. The number of holes and sparger diameter were included in the correlations developed recently.

To include the effect of sparger into correlations, ratio of hole dia, d_o, to to D was used by few investigators [Mok et. al. (1990), Mouza et. al. (2005)]. Jin et. al. (2013) used free area, number of holes, n_o, d_o and d_o/D. The gas holdup showed strong dependence on free area. Since the correlation used free area as one of the parameters, it can easily be used to correlate the data in bubble columns of square-cross section. In case of tongue type of spargers, tongue angle was also included in the correlation. Behkish et. al. (2006) took into account sparger geometry, by using n_o, d_o and D. Gas velocity based on nozzle diameter has also been attempted [Guy et. al. (1986)]. Kazakis et. al. (2007) used diameter of sparger, d_s, in one of the two dimensionless parameters d_s/D and d_o/D. The gas holdup increased with pore diameter, d_o, and sparger diameter, d_s. Anastasiou et. al. (2013) used porous plate of diameter of 0.045 m with pore diameter of 40 μm. The correlation for gas holdup was in terms of Fr, Ar, Eo, d_s/D and d_s/d_o. Sauter-mean bubble diameter, d_{32}, has also been used to represent the effect of sparger geometry indirectly [Maceiras et. al. (2010)]. Sal et al (2013) studied the effect of sparger geometry on gas holdup in an industrial size bubble column of 0.33 m diameter with perforated plate sparger with d_o = 0.001, 0.002 and 0.003 m.

Inclusion of sparger geometry in the correlation seems to be tricky as there are numerous types of spargers used in these studies. Some of these are single nuzzle,

multiple nozzle, perforated plate, ring sparger, sintered or porous plate, spider type, cross type etc.

Bukur and Patel (1989) studied gas holdup in two different columns with perforated plate, single nozzle with two different orifice sizes and sintered plate spargers. However, no single correlation could be proposed. Different correlations for pure liquids, butanol solution and CMC solutions were proposed. It indicates the difficulty in getting a single correlation due to complicated dependence of gas holdup on sparger geometry and nature of fluid. Inclusion of column diameter in the exponent of superficial gas velocity was also attempted [Degaleesan et al. (1997)]. However, such correlations are rare.

Transition from bubbly flow to heterogeneous flow and its effect on gas holdup posed problem. Under such conditions drift flux model proposed by Zahrednik et al. (1997) adequately describes the transition behaviour. This method was used later by several investigators.

2.2.2 Effect of Fluid Properties on Gas Holdup:

An examination of all the correlations for gas holdup reveals that density and viscosity of bath phases and surface tension of liquids influence gas holdup. It is reflected in appearance of several dimensionless numbers in these correlations. Electrolytic solutions, non-Newtonian fluids and coalescence inhibitors affect hydrodynamics in different ways.

Ryu et al (1993) studied performance of radial sintered sparger in a bubble column using for CMC solution. Bubbly flow and churn-turbulent flow regimes were observed. With increasing CMC concentration the behaviour was tending towards slug-flow regime. In churn-turbulent flow regime the superficial gas velocity had little effect

on gas holdup. Therefore, two correlations for both regimes were proposed. Urseanu et. al. (2003) studied gas holdup for highly viscous Newtonian fluid. The viscosity appeared in the exponent of density of the gas.

Anastasiou et. al. (2013) measured gas holdup for shear thining non-newtonian fluid in a column with porous plate sparger. For non Newtonian fluids effective viscosity was used. However, due to difficulty in measuring shear rate, it was estimated from CFD computations. The estimated values of shear rate were correlated in terms of superficial gas velocity as following:

$$\dot{\gamma} = 70 U_g^{0.48} \tag{2.1}$$

Anabtawi et. al. (2003) studied effect of column geometry on gas hold up in cylindrical and bi-dimensional bubble columns using single nozzle sparger. Due to different dependence upon superficial gas velocity, static bed height and viscosity separate corraltions were proposed for the two columns. The gas holdup decreased with increasing static bed height.

Syeda et. al. (2002) studied gas holdup for binary mixures and developed correlation based on the concept of probabilty of coalescence which itself depended on the surface tension and compistion of the mixture. In spite of several investigations it was not possible to propose a single correlation to predict gas holdup in bubble column. It was realized that sparger geometry may be an important parameter, which should be taken into account. To improve the correlation recent attempts are focussed to include the sparger geometry into the correlation.

Asgharpour et al. (2014) studied effect of addition of alkanes to water in for air-water system. It acted as bubble coalescence inhibitor by decreasing surface tension

of the liquid. As a consequence the bubble diameter decreased and gas holdup increased. The correlation used by them was dimensional and included Sauter-mean diameter as one of the parameters. To use this equation it becomes necessary to measure the value of d_{32}. However, to predict gas holdup it becomes necessary to use another correlation for d_{32}. It may be due to the fact that bubble size possibly can be taken as a measure of bubble formation and bubble coalescence.

The effect of viscosity has been always debatable though it's effect is considered to be important. Nishikawa et al. (1977) carried out heat transfer studies with Newtonian and non-Newtonian fluids. The difficulty in estimation of shear rate for non-Newtonian liquids in aerated tower was resolved by the trend of heat transfer coefficient for the both types of liquids. At superficial gas velocity, U_g, higher than 0.04 ms^{-1}, the shear rate, $\dot{\gamma}$, did not depend upon the type of the heat-transfer surface. The average shear rate for the power law fluid was used to estimate apparent viscosity, μ_0, using following equation.

$$\mu_0 = K\left(5000U_g\right)^{(n-1)} \tag{2.2}$$

where K is flow consistency index and n is flow behaviour index. At U_g < 0.04 ms^{-1}, the expressions for μ_0 for cooling coils and jackets were given by Equations (2.3) and (2.4) respectively [Nishikawa et al. (1977)].

$$\mu_0 = K\left(10000U_g^{0.5}\right)^{(n-1)} \tag{2.3}$$

$$\mu_0 = K\left(19.5U_g^{0.5}\right)^{(n-1)} \tag{2.4}$$

Based on the argument that at high gas velocity heat-transfer coefficient does not depend much upon type of the geometrical parameters and are governed by the

bubble-induced turbulence [Nishikawa et al. (1977)], same was also assumed to hold good for shear rate. Equation (2.2) has been used by various investigators to estimate apparent viscosity [Bukur and Patel (1989), Haque et al. (1987), Kantak et al. (1995)].

Schumpe and Deckwer (1987), Kawase and Kumagai (1991), and Perez et al. (2006) reviewed different approaches to estimate apparent viscosity for non-Newtonian fluids. Chisti and Moo-Young (1989) compared correlations similar to Equation (2.3) by other workers and found substantial disparity among these. The following equation, due to Henzler and Kauling, cited by Birrer and Böhm (2004) for the estimation of shear rate was based on pneumatic power input in bubble columns.

$$\dot{\gamma} = \left(P_g / \mu_0 \right)^{0.5} \tag{2.5}$$

Birrer and Böhm (2004) studied gas holdup in packed bubble column. Khamadieva and Bohm (2006) studied mass transfer in packed and unpacked bubble column. Both the works used the following expression for evaluation of apparent viscosity.

$$\mu_0 = K \left(U_g g \rho / K \right)^{(n-1)/(n+1)} \tag{2.6}$$

In case of single bubble Cordero and Zenit (2011) used the following equation for μ_0 as a function of bubble diameter, d_b.

$$\mu_0 = K \left(2U_{sb} / d_b \right)^{n-1} \tag{2.7}$$

Most of these Equations are applicable for power law fluid only.

Kawase and Moo-Young (1989) studied gas holdup in fermentation broth. The shear stress was experimentally measure and used in the correlation for gas holdup. Mok et al. (1990) measured gas holdup for CMC solution in a bubble column with

perforated plate sparger and correlated the gas holdup in terms of Reynolds number based on gas properties. The effective viscosity of non-Newtonian CMC solution was used for viscosity to estimate Galileo number in the correlation.

Fransolet et. al. (2005) studued effect of vicosity for non-Newtonian fluid using electrical resistance tomography and proposed a correlation similar to the one proposed by Godbole et al. (1982). Shear rate was taken as proportional to the superficial gas velocity.

Thakur and Rao (2007) included the effect of static bed height, H_s, as H_s/D ratio in the correlation for gas holdup. Though the dependence was week it predicted increase in gas holdup as H_s increases. Jin et al. (2007) observed the opposite trend i.e. gas holdup decreases with increasing value of H_s.

Variation of gas holdup for air-water system estimated using few earlier correlations, which did not consider the sparger geometry are compared in Fig. 2.4. It can easily been seen that there is large disagreement in the predicted values. Few of these correlations involved column diameter but it has not been possible to predict gas holdup by knowing the physical properties of the fluids used. The correlations developed for viscous and power law fluids earlier may not reliable.

Thus, it is clear that there has been large amount of uncertainty in prediction of gas holdup. Inclusion of sparger geometry improved the correlations. For non-Newtonian fluids apparent viscosity has been used in place of viscosity. However, since most of the studies used power-law fluids, a rational approach for fluids following different rheological model is required.

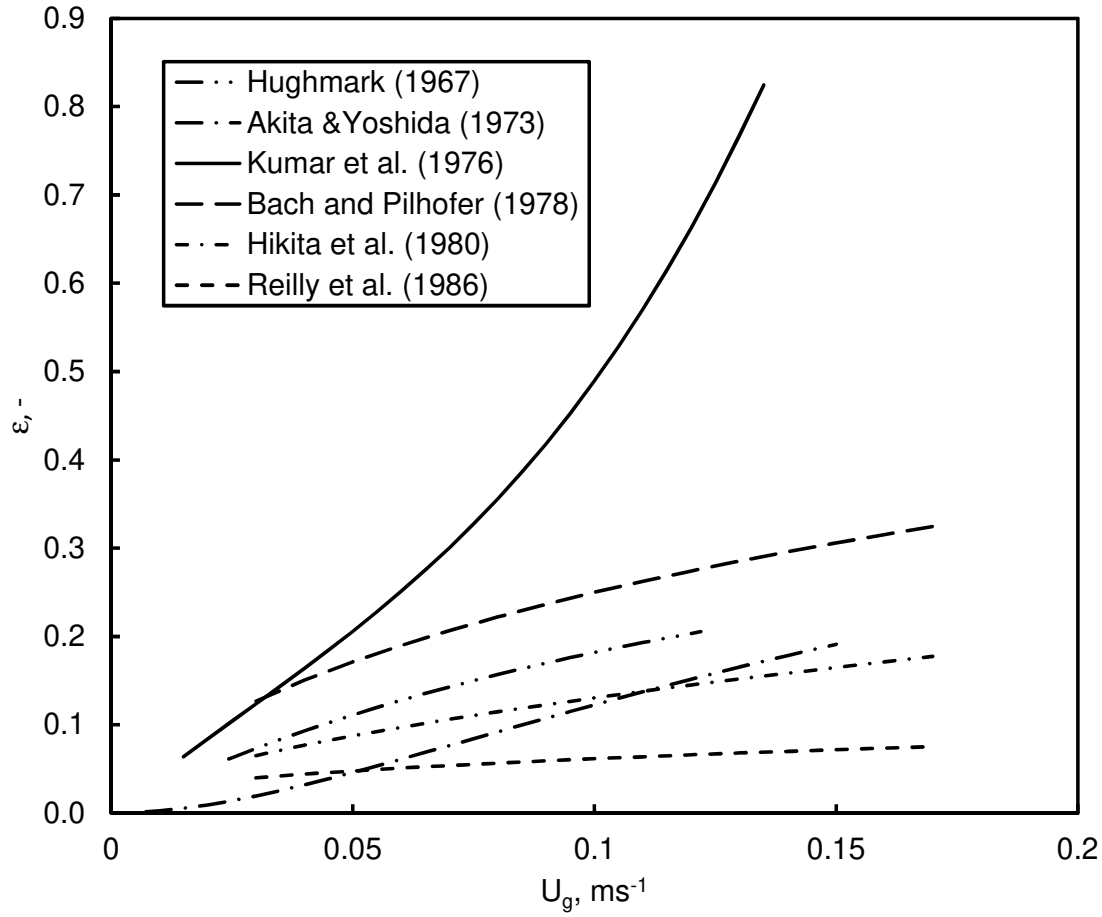

Figure 2.4: Variation of gas holdup for air-water system estimated using various correlations.

2.3 Gas-Liquid Mass-transfer Coefficient (k_La):

Gas-liquid mass transfer coefficient is often reported in terms of volumetric mass transfer coefficient, (k_La_i), which is product of mass-transfer coefficient, k_L, and specific interfacial area, a_i. Due to uncertainty in the prediction of gas holdup the approach to predict a_i from gas holdup and bubble diameter is not preferred. Thus, value of (k_La_i) were experimentally measured. Some of the correlations for (k_La_i) and Sherwood number, Sh, are presented in Table 2.2. A wide range of correlations are due to combination of k_L and a_i.

Table 2.2: Correlations for volumetric mass-transfer coefficient, $k_L a_i$ in bubble columns (PP=Perforated plate, SN=Single nozzle, SP=Sintered plate), PoP= Porous Plate, RGS= Radial Gas Sparger)

The dimensionless numbers used are Archimedes number, $Ar = D^3 \rho_l^2 g / \mu_l^2$; Eotvos number or Bond's Number, $Eo = Bo = gD^2 \rho_l / \sigma_l$;

Morton number, $Mo = \mu_l^4 g / \rho_l \sigma^3$; Reynold's number, $\mathrm{Re} = DU_g \rho_l / \mu_l$; Froude number, $Fr = U_g / \sqrt{gD}$; ; Galileo Number, $Ga = gD^3 \rho_l^2 / \mu_l^2$

Investigator	Correlation	System	Column
Akita and Yoshida (1973)	$k_L a_i D^2 / D_L = 0.6 Sc^{0.5} Bo^{0.62} Ga^{0.21} \varepsilon^{1.1}$	Air, oxygen, helium/water, glycol, glycerol, methanol, 0.15M Sodium sulphite solution	D=0.152, 0.301, 0.6 m d_o=0.005 m, n_o = 1
Akita and Yoshida (1974)	$Sh = \left(k_L d_{vs} / D_L\right) = 0.5 Sc^{1/2} Bo^{3/8} Ga^{1/4} \varepsilon^{1.1}$	Air, water, glycol (30,70,100%), glycerol (25,45,65%), methanol, Sodium sulphite solution (0.15M)	Square Cross Section (0.15 m^2) PP[(d_o=0.0004 m, n_o = 52,105,247), [(d_o=0.0006 m, n_o = 52,105,247), [(d_o=0.0008 m, n_o = 52,105,247), [(d_o=0.001 m, n_o = 27,52,105,247), [(d_o=0.002 m, n_o = 247) PoP(0.00012-0.0001, 0.00005-0.00005, 0.00003-0.00002, 0.00001-0.000005 m) Square Cross Section [D=0.077 m^2 (SN d_o=0.003 m), D=0.15 m^2 (SN d_o=0.001, 0.002, 0.0045 m), D=0.2 m^2 (SN d_o=0.005 m)]

Schumpe and Deckwer (1982)	$k_L = 0.0045 U_G^{-0.08} \mu_{eff}^{-0.32}$	Air, CMC (0-2%) Na_2SO_4 (0.8mol/l)	D=0.102, 0.14 m SP (d_o=0.00015, 0.0002 m) PP [(d_o=0.0005 m, n_o=421), (d_o=0.001 m, n_o=73), d_o=0.002 m, d_o=19)]
Sada et.a l. (1985)	$k_L = 0.014 U_G^{-0.86}$ $k_G = 170 U_G^{0.72}$	O_2/ NaCl, NaOH, $Ca(OH)_2$ 5% CO_2/ NaCl, NaOH, $Ca(OH)_2$	D=0.05 m PP (d_o=0.001 m, n_o=10)
Sada et. al. (1986)	$k_L a = 0.24 \varepsilon^{0.9}$	Ion-exchanged water, Sucrose, Na_2SO_4, NaCl, KCl, $Ca(OH)_2$, glass bead, nylon6, pure O_2, N_2	D=0.078 m PP (d_o=0.001 m, n_o=37)
Ryu et. al. (1993)	$k_L a_i D^2 / D_L = 4.95 x 10^7 Sc_{eff}^{-0.31} Fr^{0.16}$ For bubbly flow $k_L a_i D^2 / D_L = 5.8 x 10^7 Sc_{eff}^{-0.345} Fr^{0.495}$ Churn-turbulent flow	Air, CMC (0.7 wt. %)	D=0.115 m RGS ((D_S=0.038 m, H_S=0.15 m, d_o=5 µm
Alvarez et. al. (2000)	$k_L a_i = K_1 U_g^{2/3} \sigma^{3/4} \mu_l^{-3/4} \rho_l^{3/2}$ 1.924x10^{-7}, 1.969x10^{-7}, 2.079x10^{-7} for different plates	Pure CO_2, Sucrose and Sodium Lauryl Sulphate Solution	D_i=0.113, D_o=0.148 m PoP (150-200, 90-150, 40-90 µm)
Vazquez et. al. (2000a) Vazquez et. al. (2000b)	$k_L = K_1 \sigma^{1.35} U_g^{0.5}$; K_1 depends upon sparger	Pure CO_2, Water, Buffer solution Na_2CO_3-$NaHCO_3$, Sodium Arsenite (Catalyst), SLS	D_i=0.113, D_o=0.148 m PoP (150-200, 90-150, 40-90 µm)
Jordan and Schumpe (2001)	$Sh = a_1 Sc^{0.5} Bo^{0.34} Ga^{0.37} Fr^{0.72} \left[1 + 13.2 Fr^{0.27} \left(\rho_g / \rho_l\right)^{0.49}\right]$ a_1= constant depending upon sparger	N_2, He, Ethanol(96%),1-Butanol, Toluene, Decalin	D=0.1 m, PP (d_o=0.0043 m, n_o=1, d_o=0.001 m, n_o=1, d_o=0.001 m, n_o=19

Behkish et. al. (2006)	$k_L a_i = 0.18 Sc^{0.6} \left(\rho_l \nu_A / M_B\right)^{-2.84} U_g^{0.553} \left(\rho_g U_g\right)^{0.49} \exp\left(-2.66 C_{SV}\right)$ C_{SV}- volumetric solid conc.		Data available in literature is used for correlations
Hughmark (1967)	$\left(k_L d_{32} / D_L\right) = 2 + 0.0187\,\mathrm{Re}^{0.779}\, Sc^{0.546} \left(d_{32} g^{1/3} / D_L^{2/3}\right)^{0.116}$	Air/water, Versol, Glycerol, Na_2CO_3 soln., $ZnCl_2$ soln.	D=0.0254, 0.0508, 0.1524, 0.3048m
Baz-Rodriguez et. al. (2014)	$k_L / k_{Lw} = \left(1-\varepsilon\right)^{4.377} \left[2.12 Eo^{0.1906} - \exp\left(0.009016 c_r^2\right)\right]$	Air, NaCl (0.05, 0.13, 0.21, 0.29, 0.37 M), $CaCl_2$ (0.02, 0.04, 0.06, 0.08, 0.10 M), $MgCl_2$ (0.02, 0.04, 0.05, 0.08, 0.11, 0.14)	D=0.095 m, PoP (d_o= 160-250 μm)
Jin et. al. (2014)	$k_L a_i = 3.051 \times \left(\rho_l \nu_A / M_B\right)^{-1.193} Sc^{-0.734} \left(\rho_g U_g\right)^{0.524}$	H_2, CO, CO_2, paraffin, sand (particle size 150-200 μm)	D=0.1 m, PP (d_o=0.008 m, n_o=4)
Zhao et. al. (2004)	$\ln(k_L) = 4.13 + 0.797 \ln(\sigma) + 0.411 \ln(U_g) - 2.59 \times 10^3 / T$	CO_2, Na_2CO_3-$NaHCO_3$ (0.5 mol/L) $NaAsO_2$ (0-0.008 mol/L, catalyst), DBS (0-5 mg/L, surface tension modifier)	D=0.102 m,
Bhatia et. al. (2004)	$Sh = 2.0 + 0.6\,\mathrm{Re}^{0.5}\, Sc^{0.33}$	Air, Tap Water, alcohol ((0.5 volume %)	D=0.2 m, PP (d_o=0.0025 m, n_o=1256)
Therning and Rasmuson (2006)	$k_L a_i = k_M\, D_L / D\, Sc^{0.5} Bo^{4/7} Ar^{2/7} \varepsilon^{1.18}$; k_M depends upon surface conc.	Air, deionized water,Na_2SO_3 (0.8 M), H_2SO_4 (0.06-0.035 M)	D=0.2 m, PP (d_o=0.002 m, n_o=69) D=0.05 m, PoP (d_o=5 μm, Plastic membrane)
Nedeltchev et. al. (2007)	$k_L a = f_c \sqrt{4 D_L R_{sf} / \pi S_B}\left(f_B S_B / A U_B\right)$ where $R_{sf} = \pi \sqrt{\left(l^2 + h^2\right)/2 - \left(l-h\right)/8}.U_b$ and $f_c = 0.124 Eo^{0.94} \left(\rho_G / 1.2\right)^{0.15}$		
van der Schaaf et. al. (2007)	$k_L a_i / \varepsilon = 3.0 \sqrt{D U_b / d_b^3}$	Air, N_2, Demineralized water, organic oil (Isopar	D=0.15 m PP(D = 0.1 m, d_o= 0.0005

		M, Exxon-Mobil)	m)
Thaker and Rao (2007)	$k_L a_i = 1.87 U_g^{0.56} \left(H_s / D \right)^{-1.68}$	Pure CO_2, distilled water, Aqueous NaOH solution (1N)	D=0.14 m PP (d_o=0.001 m, n_o=24)
Gomez-Diaz et. al. (2009)	$k_L a_i = 0.85 U_g^{1.2} \eta_{eff}^{-0.1}$	CO_2, k-carrageenan distilled water solution	D=0.07 m
Asgharpour et. al. (2010)	$Sh = 0.15 \mathrm{Re}^{2/3} Sc^{1/2} Bo^{2/3}$	Air, Distilled water (n-decane, n-tridecane, n-hexadecane used as impurities)	D=0.095 m PP (d_o=0.0003 m, n_o=26)

D_S=Sparger Diameter (m), H_S=Sparger Height (m), d_o=Orifice Diameter (m), n_o=Number of Openings, D=Column Diameter (m), D_i=Inside Tube Diameter (m), D_o=Outside Tube Diameter m

Column diameter has been the only geometrical parameters considered in the correlations for (k_La_i) [Hughmark (1967), Akita and Yoshida (1973)]. The latter proposed correlation in terms of dimensionless numbers Sc, *Bo* and *Ga*, each of these may be estimated using physical properties of the fluids. Hughmark (1967) and Akita and Yoshida (1974) studied effect of bubble size on k_La_i. Schumpe and Deckwer (1982) measured specific interfacial area and using it in the correlation for (k_La_i) proposed by Deckwer et al. (1982) to obtain an expression for k_L. It did not include any physical propery of the fluid except effective viscosity.

The dependence of (k_La_i) on sparger geometry has resulted in different constants for bubble columns with different sparger geometry [Alvarez et al. (2000), Jordan and Shumpe (2001), Vezquez et al. (2000a, 2000b)]. Ryu et. al. (1993) proposed two correlations for (k_La_i) depending upon the type of flow i.e. bubbly flow and churn-turbulent flow. It was concluded that sparger type has great impact on values of k_La_i. Since, sparger geometry influences gas holdup also, expressing (k_La_i) in terms of gas holdup may be considered as if sparger geometry is indirectly taken into account. Table 2.2 lists some of these correlations [Sada et. al. (1986); Akita and Yoshida (1973; 1974);Therning and Rasmuson (2006); Schaaf et. al. (2007)]. Correlation by Schaaf et. al. (2007) requires bubble size and bubble rise velocity also to predict (k_La_i). Correlation by Thaker and Rao (2007) requires static bed height on (k_La_i) in the correlation and predicts k_La_i to decrease with increase in static bed height.

A few attempts have also been to apply mass trasnfer theories in bubble columns. Nedeltchev et. al. (2007) proposed a correction factor to penetration theory to correlate data on mass-transfer coefficient in bubble columns operated at high pressure.

It is well known that ($k_L a_i$) can be estimated by knowing mass-trasnfer coefficient and a_i. However, such attempts are not many possibly due to complex nature of the bubble column and a large number of variables involved. It may be interseting to study the effect of sparger on k_L and a_i separately and search for a more reliable correlation.

Based on the above discussion it is clear that $k_L a_i$ depends on the value of a_i, which strongly depends upon the nozzle diameter. For better correlation of a_i, it is necessary to study dependence of bubble diameter on other variables. Bubble size measurement to obtain BSD is essential to have a good estimate of a_i. Bubble size is also related to bubble velocity and hence induced turbulence. Thus, bubble size is an important parameter, which may be important while estimating mass-transfer coefficient.

2.4 Bubble Diameter:

A vast literature on Bubble diameter in gas-liquid systems is available. Bubble diameter in bubble column has also been studied by several investigators. Some of the correlations are presented in Table 2.3 Bubble diameter depends upon the size of bubble at the time of formation, their growth due to coalescence and reduction in size due to bubble breakup during its stay in the column. When bubble breakup dominates in comparison to bubble coalescence, the bubble size at the time of formation of bubble at the tip of the nozzle is not important. Under such conditions, the nozzle diameter will have insignificant or negligible effect on the bubble size. Correlation of Akita and Yoshida (1974) did not find effect of nozzle diameter on bubble size. It may be an indication that bubble breakup determined the bubble size. Hinze (1955) developed an equation based on turbulence to estimate maximum diameter of bubble.

Table 2.3: Correlations for bubble diameter, d_{32} in bubble columns The dimensionless numbers used are Archimedes number, $Ar = D^3\rho_l^2 g/\mu_l^2$; Eotvos number or Bond's Number, $Eo = Bo = gD^2\rho_l/\sigma_l$; Morton number, $Mo = \mu_l^4 g/\rho_l\sigma^3$; Reynold's number, $\mathrm{Re} = DU_g\rho_l/\mu_l$; Froude number, $Fr = U_g/\sqrt{gD}$; ; Galileo Number, $Ga = gD^3\rho_l^2/\mu_l^2$

Investigator	Correlation	System	Column
Akita and Yoshida (1974)	$d_{32}/D = 26Bo^{-0.5}Ga^{-0.12}Fr^{-0.12}$	Air, water, glycol (30,70,100%), glycerol (25,45,65%), methanol, Sodium sulphite solution (0.15M)	Square Cross Section (0.15 m^2) PP[(d_o=0.0004 m, n_o = 52,105,247), [(d_o=0.0006 m, n_o = 52,105,247), [(d_o=0.0008 m, n_o = 52,105,247), [(d_o=0.001 m, n_o = 27,52,105,247), [(d_o=0.002 m, n_o = 247) PoP(0.00012-0.0001, 0.00005-0.00005, 0.00003-0.00002, 0.00001-0.000005 m) Square Cross Section [D=0.077 m^2 (SN d_o=0.003 m), D=0.15 m^2 (SN d_o=0.001, 0.002, 0.0045 m), D=0.2 m^2 (SN d_o=0.005 m)]
Kumar et. al. (1976)	For $1 < Re < 10$ $d_{32} = 1.56(\mathrm{Re})^{0.058}\left(\sigma d_o^2/\Delta\rho_l g\right)^{1/4}$ For $10 < Re < 2100$ $d_{32} = 0.32(\mathrm{Re})^{0.425}\left(\sigma d_o^2/\Delta\rho_l g\right)^{1/4}$	Air, Water, Glycerol (40%),, Kerosene CO_2, Aqueous NaOH (2M)	D=0.05, 0.075, 0.1 m SN (d_o=0.00087, 0.00153, 0.00196, 0.00265, 0.00309 m, n_o=1)

	For 4000 < *Re* < 70000 $d_{32} = 100(\mathrm{Re})^{0.4}\left(\sigma d_o^2/\Delta\rho_l g\right)^{1/4}$		
Gaddis and Vogelpohl (1986)	$d_b = \left[\left(\frac{6d_o\sigma}{\rho_l g}\right)^{4/3} + \left(\frac{81\mu_l Q_o}{\pi g \rho_l}\right) + \left(\frac{135Q_o^2}{4\pi^2 g}\right)^{4/5}\right]^{1/4}$	Air, Water, Glycerol	SN (d_o=0.0002-0.006 m, n_o=1)
Hinze (1955)	$d_b = 0.725(\sigma/\rho_l)^{0.6}(U_o g)^{-0.4}$		
Walter (1983)	$d_b = (\sigma/\rho_l)^{0.6}(\mu_l/\mu_g)^{0.1}(U_o g)^{-0.4}$		
Pohorecki et. al. (2005)	$d_{32} = 0.289\rho_l^{-0.552}\mu_l^{-0.048}\sigma^{0.442}U_g^{-0.124}$	Air, Acetaldehyde, Acetone, Cyclohexane, Isopropanol, Methanol, N-Heptane, Toluene N_2, Cyclohexane, Water	D=0.09, 0.304 m PP (d_o=0.001-0.005 m, n_o=1-27)
Jamialahmadi et. al. (2001)	$d_b/d_o = \left[\left(\frac{5.0}{Bo_b^{1.08}}\right) + 9.261\left(\frac{Fr^{0.36}}{Ga^{0.39}}\right) + 2.147Fr^{0.51}\right]^{1/3}$		
Mok et. al. (1990)	$d_b(\rho_l g / d_o\sigma)^{1/3} = 2.61\left(We / Fr^{0.5}\right)^{0.182}$	Oil free Air, Water, CMC (0.05, 0.075, 0.1, 0.15, 0.2, 0.3 wt%)	D=0.14 m PP (d_o=0.0003 m, n_o=51)
Pohorecki et al. (1999, 2001)	$d_{32} = 1.658\times10^{-3}U_g^{-0.12}$	N_2, Cyclohexane	D=0.304 m PP (d_o=0.001-0.005 m, n_o=1-27)
Jamshidi and Mostoufi (2018)	$\frac{d_b^{'}}{D} = 3.85*10^2 Fr^{0.7}Ga^{-0.2}Bo^{-0.3}$	Air, water, CMC	D = 0.09 m, H = 1.75 m, PP(no = 100, do = 0.0005 m)

Kanaris et. al. (2018)	$\frac{d_{32}}{D} = 0.9\left[We^{0.95}\,\mathrm{Re}^{0.40}\,Fr^{0.47}\left(\frac{d_o}{D}\right)^{0.55}\right]^{0.51}$	Air, CO_2, He, water, glycerin	PoP(0.00004 m, 0.0001m)
Mouza (2018)	$\frac{d_{32}}{d_s} = 12.5\left[We^{-15.87}\,\mathrm{Re}^{13.73}\,Fr^{9.19}\left(\frac{d_o}{d_s}\right)^{2.77}\right]$	Air, water, glycerine, butanol, xanthan gum	PoP(0.00004 m, 0.0001 m)
Azizi et. al. (2019)	$d_i = 2.19*10^{-9} d_o\,\mathrm{Re}_{d_o}^{1.46}\,Eo_{d_o}^{-0.52}$ $d_m = 6.75*10^{-6}\frac{\sigma^2}{g\mu_l^2}\left(\frac{D}{n_o\delta_p}\right)^{0.47}\mathrm{Re}_{d_i}^{0.34}$	Air, water	D = 0.1 m, H = 1 m, Needles(n_o = 13, 19, 31, 42, 73, 115), (δ_p = 0.027, 0.021, 0.016, 0.014, 0.009, 0.008 m)
Feng et. al. (2019)	$\frac{d_{32}}{D} = 0.35\left[We^{0.95}\,\mathrm{Re}^{0.40}\,Fr^{0.47}\left(\frac{d_o}{D}\right)^{0.55}\right]^{0.09}$	N_2, He, water, ethanol	D = 0.01 m, H = 0.1 m SN (d_o=0.00008, n_o=1)

Pohorecki et al. (2001) carried out numerical experiment and proposed the following equation for bubble diameter after validating the equation for 7 organic solvents.

$$d_{32} = 0.289\rho^{-0.552}\mu^{-0.048}\sigma^{0.442}U_g^{-0.124} \tag{2.8}$$

Equation (2.8) predicts bubble diameter to decrease with increasing superficial gas velocity. It seems that bubble breakup determined bubble size.

Correlation by Kumar et al. (1976) considers effect of nozzle diameter. It indicates that bubble formation at the nozzle has an effect on the bubble size. The effect of nozzle diameter might be changing with Reynolds number, as it is indicated by three different correlations for different range of Reynolds number. Gaddis and Vogelpohl (1986) considered flow rate through a single nozzle as a parameter combining flow rate and nozzle diameter as one parameter in addition to nozzle diameter. Several other correlation also requires nozzle diameter to estimate bubble size [Jamialahmadi et. al. (2001); Mok et al. (1990); Kanaris et. al. (2018); Feng et. al. (2019); Mouza (2018)]. These studies show that bubble breakup does not dominates. However, it does not clearly allow us to distinguish between the importance of bubble formation and bubble coalescence. It may be due to combination of both.

In literature contrary conclusions have been reported. Pohorecki et al. (1999) observed that value of d_{32} is constant. Later Pohorecki et al. (2001) carried out numerical experiment and observed that d_{32} decreases with increasing U_g. Similar result has been reported by Akita and Yoshida (1974).

While Kanaris et. al. (2018) and Feng et. al. (2019) expressed d_{32}/D as a function of We, Re, Fr and d_o/D, Mouza et al (2018) used d_{32}/d_o and d_{32}/d_o. Jamshidi and Mostoufi (2017) proposed a correlation for ratio of maximum bubble chord length to column diameter. Aziz et. al. (2019) proposed correlations for initial bubble size and

mean bubble size in terms of Re, Eo and sparger geometry parameter, n_o and pore diamter δ. The dimensionless numbers were estimated for gas velocity at the nozzle,

A close review of the correlations presented in Table 2.3 and the discussion above it is clear that the nozzle diameter seems to be an important parameter for estimation of bubble diameter. The relationship between the two may depend upon the flow regime. If bubble diameter changes due to bubble coalescence and bubble breakup, while the bubble move up, it will be interesting to study variation of bubble size with increasing distance above the sparger.

It is important to notice that bubble diameter, d_b, and Sauter-mean bubble diameter, d_{32}, are not same. However, both can be determined from bubble size distribution.

2.5 Specific Interfacial Area:

Specific interfacial area in bubble columns has been reported by several investigators. It is easily estimated from the value of d_{32}. Interfacial area has been defined in literature two ways. Earlier specific interfacial area was estimated as surface area per unit volume of gas-liquid dispersion [Pohorecki et al. (1999), Buchholz et al. (1979), Ryu et al. (1993)].

$$a_i = 6\varepsilon / d_{32} \tag{2.9}$$

Recently specific interfacial area is being estimated as surface area per unit volume of liquid [Bouaifi et al. (2001), Díaz et al. (2009), Maceiras et al. (2010)].

$$a_i = 6\varepsilon / d_{32}\left(1-\varepsilon\right) \tag{2.10}$$

The specific interfacial area defined by Equation 2.9 is required for reactor design.

Table 2.4: Correlations for specific interfacial area, a_i in bubble columns

Investigator	Correlation	System	Column
Akita and Yoshida (1974)	$a_i D = (1/3)\, Bo^{0.5} Ga^{0.1} \varepsilon^{1.13}$	Air, water, glycol (30,70,100%), glycerol (25,45,65%), methanol, Sodium sulphite solution (0.15M)	Square Cross Section (0.15 m^2) PP[(d_o=0.0004 m, n_o = 52, 105,247), [(d_o=0.0006 m, n_o = 52,105,247), [(d_o=0.0008 m, n_o = 52,105,247), [(d_o=0.001 m, n_o = 27, 52, 105, 247),[(d_o=0.002 m, n_o = 247) PoP(0.00012-0.0001, 0.00005-0.00005, 0.00003-0.00002, 0.00001-0.000005 m) Square Cross Section [D=0.077 m^2 (SN d_o=0.003 m), D=0.15 m^2 (SN d_o=0.001, 0.002, 0.0045 m), D=0.2 m^2 (SN d_o=0.005 m)]
Kumar et. al. (1976)	For 100 < Re_o<2100 $a_i \mathrm{Re}_o^{0.425} \left(\frac{\sigma d_o^4}{\Delta \rho_l g} \right)^{1.4} = 13.650 U_g^* - 9.094 U_g^{*2} + 1.828 U_g^{*3}$ For 4000< Re_o <70000 $a_i \mathrm{Re}_o^{-0.4} \left(\frac{\sigma d_o^4}{\Delta \rho_l g} \right)^{1/4} = 0.0437 U_g^* - 0.091 U_g^{*2} + 0.0059 U_g^{*3}$	Air, Water, Glycerol (40%),, Kerosene CO_2, Aqueous NaOH (2M)	D=0.05, 0.075, 0.1 m SN (d_o=0.00087, 0.00153, 0.00196, 0.00265, 0.00309 m, n_o=1)

Schumpe and Deckwer (1982)	$a_i = 4.65\times10^{-2} U_G^{-0.51} \mu_{eff}^{-0.51}$; for slug flow only	Air, CMC (0-2%) Na_2SO_4 (0.8mol/l)	D=0.102, 0.14 m SP (d_o=0.00015, 0.0002 m) PP [(d_o=0.0005 m, n_o=421), (d_o=0.001 m, n_o=73), d_o=0.002 m, d_o=19)]
Chen et. al. (2008)	$a_i = 9271 U_G^{1.09}$	N_2-CO_2 mixture, water, $BaCl_2$, NaOH, $BaCO_3$	D=0.05 m PP (d_o=0.001 m, n_o=4/square cm)
Zhao et. al. (2004)	$a_i = 1480\sigma^{-0.00130} U_G^{0.634} e^{292/T}$	CO_2, Na_2CO_3-$NaHCO_3$ (0.5 mol/L) $NaAsO_2$ (0-0.008 mol/L, catalyst), DBS (0-5 mg/L, surface tension modifier)	D=0.102 m
Pohorecki et al. (1999)	$a_i = 1120 U_g^{0.63}$	N_2, water	D = 0.3 m, PP(d_o=0.001 m - 0.005 m, n_o= 1 - 27)
Bouaifi et al. (2001)	$a_i = 0.26\left(P_G/V_L\right)^{0.63} = 0.26\left(\rho_L g U_G\right)^{0.63}$	Air, water	D = 0.43 m, RGS (D_S=0.165 m, d_o=0.001 m, n_o= 90)
Lau et al. (2012)	$a_i = 18(1.208)\varepsilon \Big/ \left[(1-\varepsilon)\exp\left(\alpha-(5/2)\beta^2\right)\right]$	Air/N_2-O_2 mixtue	D = 0.14 m, PP(d_o=0.003 m, n_o= 211), SP(d_o=0.0006 m) ,SN (d_o=0.055 m)
Besagni and Inzoli (2017)	$a_i = (0.23/D)\, AR^{-0.3} Eo^{1/2} Ga^{0.12} Fr^{1/2}$	Deionized water, Aq. Soln of NaCl, Etanol and MEG	D=0.24; $5 \le AR(=H_o/D) \le 12.5$;
Vazquez et. al. (2000)	$a_i = 0.0046\,\mathrm{Re}^{0.98} Fr^{0.19} Bo^{-0.70} Sc^{0.57} \left(d_o/D\right)^{-0.19}$	Pure CO_2, Water, Buffer solution Na_2CO_3-$NaHCO_3$, Sodium Arsenite (Catalyst), SLS	D_i=0.113, D_o=0.148 m PoP (150-200, 90-150, 40-90 µm)

Correlations for interfacial area are presented in Table 2.4. Correlation by Schumpe and Deckwer (1982), for slug flow regime, predicts a_i to decrease of with increasing effective viscosity. Correlations by Akita and Yoshida (1973) and Sada et al (1984) involved Bo and Ga. The values of a_i depend upon column diameter, D and gas holdup. The latter indirectly takes into account effect of sparger.

Pohorecki et al. (1999) compared several correlations to predict the values of a_i and found that a_i increases with increasing U_g. Vazquez et. al. (2000) correlated their data in terms of Re, Fr, Bo, Sc and d_o/D. The Fr in their correlation was square of the Fr used by most of the investigator. Bouaifi et al (2001) proposed a_i to be proportional to power dissipated in a bubble column, $P_G/V_L = \rho_L g U_G$.

Lau et al (2012) measured bubble size distribution in a shallow bubble column. The data were fitted with log-normal distribution. An expression for interfacial area in terms of paramaters associated with bubble-size distribution was proposed. Correlation proposed by Bouaifi et al (2001) considered a_i to be proportional to the power dissipated in a bubble column, P_G/V_L which is equal to $\rho_L g U_G$.

Estimated values of specific interfacial area for air-water system using correlations of Akita and Yoshida (1974), Pohorecki et al. (1999), Bouaifi et al (2001), Zhao et al. (2004) and Chen et al. (2008) are presented in Figure (2.5). These correlations did not require nozzle diameter. Estimations were made only for the range for which respective correlations were proposed.

All the equations predict increasing interfacial area with increasing gas velocity. Correlation proposed by Bouaifi et al (2001) , Zhao et al. (2004) and Pohorecki et al. (1999) were based on the data in a narrow range of gas velocity. Data of Chen et al (2008) covered a wide range of gas velocity and predicted values of interfacial area are

comparable. Correlations of Bouaifi et al (2001) , Zhao et al. (2004) predict much higher values of interfacila area than that predicted by correlation Chen et al (2008). Correlation of Pohorecki et al. (1999) are comparable to the latter. Values predicted by Akita and Yoshida (1974) are about 50% of the values predicted by correlation of Chen et al (2008).

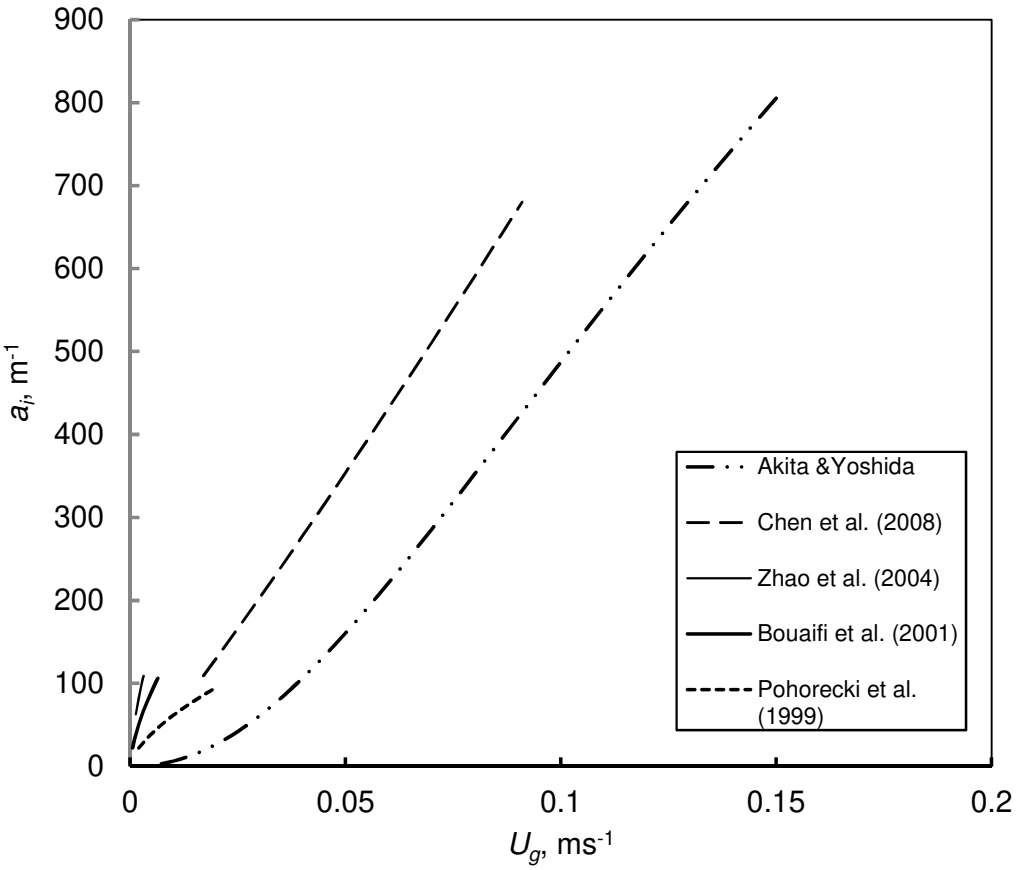

Figure 2.5: Variation of interfacial area for air-water system estimated using various correlations.

Based on the above discussion it is clear that volumetric mass-transfer coefficient depends on specific interfacial area, which strongly depends upon the nozzle diameter. For better correlation of specific interfacial area it is necessary to study the variation of bubble diameter. Bubble size measurement to obtain bubble-size distribution is essential to have a good estimate of specific interfacial area. Bubble size is also related to bubble velocity and hence induces turbulence, which may give an estimate of mass-transfer coefficient.

Selection of a suitable measuring technique is an important aspect of experimental studies. A few of the desirable qualities are non-intrusive and non-invasive nature of the technique, fast response, cost effectiveness, ability to sense tiny bubbles etc. In the following section some of the techniques tried in bubble columns are briefly presented.

2.6 Measurement Techniques for Bubble Behaviour:

A number of techniques have been applied to study the hydrodynamics of bubble column. Commonly used hydrodynamics study techniques are classified according to their working principle. These techniques may be broadly classified as photographic, Tomography, Radiography, Probe-Technique, acoustic etc.

2.6.1 Visualization Techniques:

Visualization techniques refer to methods of obtaining images or video by using high quality camera at high recording speed and analysing the images to obtain various hydrodynamic parameters. A brief account of these is mentioned in the following section.

2.6.1.1 High Speed Photography (HSP): Photographic technique for measurement is a non-instructive direct technique for measurement of bubble size

distribution. The bubbles may be counted and their shape and sizes can be measured. Akita and Yoshida (1974) used photographic method to study, bubble size and interfacial area in a two-dimensional bubble column. Though this technique is a direct technique but it requires the wall to be transparent. The technique is slow and not suitable for online measurements. The HSP technique is cheap, easy and gives accurate values. This technique was earlier time taking due to manual analysis of frame-by-frame analysis but now with application of suitable image processing techniques the time of analysis has considerable decreased. Transparent medium as well as vessel should be required for the application of this technique.

De Swart et al. (1996) studied the hydrodynamics of two-dimensional slurry bubble column using photographic technique. Experiments were conducted with air/paraffin oil slurries with solids concentrations of 0, 28.3 and 38.6 volume per cent of porous silica particles. Bubble-size, bubble coalescence and bubble break up rates were determined by video image analysis. The coalescence and break up rates were determined by frame-by-frame analysis of the video recording. The video signals produced by the camera were digitized at a rate of 25 frames per second. The real-time signals were directed to a video monitor for online control of the camera output. The captured images were transferred and processed to a PC. The true colour image was converted to grey colour images and each pixel (equal to 1mm) was analysed. Use of PC and suitable image processing software was helpful in online measurement using photographic techniques. The properties such as area, width and height were measured. The equivalent bubble diameter was calculated directly from the bubble area.

Low gas phase concentration, transparent column and proper light with undisturbed medium between camera and column are necessary for applying optical imaging technique. Dominance of large bubbles over small bubbles, resolution of the

camera and sensitivity of the CCD cell cannot be neglected for determination of bubble size. Similarly Bubble Size Distribution is strongly dependent on edges and overlapping.

2.6.1.2 Dynamic Gas Disengagement Technique: Srifam and Mann (1977) first proposed Dynamic Gas Disengagement technique (DGDT) to determine the bubble size distribution in a bubble column. In this simple technique, liquid level in the column is decreased by disconnecting the gas flow suddenly with the help of a Solenoid valve after the system reaches steady state at a given superficial gas velocity. The decrease in liquid level was recorded from a vertical ruler fitted next to the bubble column with the help of a Video Camera and a Video Cassette Recorder unit. The fall of liquid level is plotted as a function of time that shows the larger and smaller sized bubbles fractions in the column. The drastic fall of the liquid level causes the steep slope in the graph due to disappearance of bubbles of larger size whereas the slight slope is referred towards the contribution of the smaller size bubbles.

The applications of the DGDT is found in the hydrodynamics study of bubble column for determination of the gas hold up, bubble rise velocities, surface area, residence time distribution of the gas phase and its mixing intensity, to find the shape and rising velocity of bubbles and to calculate the average Sauter mean diameter for the whole column [Deshpande et al. (1995), Fransolet et al. (2005)] compared bubble size distributions for both Newtonian and non-Newtonian fluids determined by gas disengagement technique using five parietal pressure probes.

2.6.2 Probe Techniques:

These are interactive techniques in which an external direct or indirect measuring probe is being inserted into the bubble column in order to collect the

required signal to study the hydrodynamics. In these cases there are chances of disturbances of the main flow pattern inside the column because of the external probes.

2.6.2.1 Optical Probe: Optical Probe (OP) is probably the first technique that used transmission of light for measuring the bubble size, its frequency and rise velocity in fluidized beds. To study the bubble size and its growth this technique can also be applied (Rudisuli et al., 2012). This technique is used for measurement of local gas holdups and chord lengths in a bubble column [Pjontek et al. (2014), Chaumat et al. (2007)].

2.6.2.2 Resistivity Probe: The basis of Resistivity Probe (RP) is that, when a voltage of a certain frequency is supplied to the needles, the amplitude of the output signal changes as different phases passed through the probe tip [Shiea et al. (2013)]. It is a simple technique for identification of passage of interface near the probe tip and for determination of bubble velocity, bubble size and gas hold up [Sanaullah et al. (2001)]. It can be used to study flow regimes (dispersed bubble flow, discrete bubble flow, coalesced bubble flow and slug flow) and to prepare the flow regime map [Shiea et al. (2013)].

2.6.2.3 Conductivity Probe: The Conductivity or Capacitance Probe is based on the electrical conductance differences between different phases in the system. Bubble properties valuations, instantaneous gas holdup measurements and for transitions regime estimation were obtained [Gupta et al. (2000)]. This technique is also utilized to measure bubble dynamic parameters and liquid slug length in the Taylor flow regime [Yuan et al. (2012)]. The conductivity probe technique allows higher sampling rates [Hoppe et al. (2010)]. With this technique only localized information can be found and this method cannot distinguish the components of the velocity vector. Due

to bubble deformation occurring at high gas holdup causes large errors in the application of conductivity probe [Liu et al. (2007)]. Use of conductivity probe is also limited due to hitting of bubbles to the probe that corrupts the measured signal [Gupta et al. (2000)].

2.6.2.4 Capillary Suction Probe: In Capillary Suction Probe technique, a small, thin capillary is located inside the bubble column through which dispersion is sucked applying slight vacuum at capillary outlet. Thus, the sucked gas–liquid dispersion particles transform into cylindrical slugs of equivalent volume. The technique has been used to measure local bubble sizes and bubble size distribution in a double turbine agitated vessel [Alves et al. (2002)] and to investigate local gas holdup of bubble columns using the bubble slug lengths and their intervals [Barigou and Greaves (1991); Yang and Wang (1991); Alves et al. (2002); Du et al. (2003)]. It can not be used to measure size of small bubbles.

2.6.3 Cross Sectional Wire Mesh (CSWM):

The CSWM measurement technique was first implemented by Johnson to measure the gas fraction [Prasseret al. (2005)]. It consists of two grids of parallel isolated wires crossing at right angle to each other placed over the measurement cross-section. The instantaneous electrical conductivity at the intersection points of the two wires of the wire mesh sensor differ due to the passage of different phases of the mixture which is the basis of the CSWM technique [Nuryadin et al. (2015). This technique gives complete information of two-phase flow structure and void fraction profiles avoiding use of complicated algorithms [Prasseret al., (2001)]. Due to intrusive nature it is not suitable at low flow velocities [Beyer et al. (2010); Zhang et al. (2013)].

2.6.4 Laser Doppler Anemometry:

The technique is based on the principle of Doppler effect [Boyer et al. (2002)]. It has been used for measurement of size of gas bubble and liquid droplets, bubble distributions and bubble rise velocity [Mudde et al. (1997); Kulkarni et al. (2001); Brenn et al. (2002)]. PDA measures the velocities from which the bubble collisions probability can be predicted [Brenn et al. (2002)]. Olmos et al. (2003) studied the structures and observed the two states (un-established and fully established) of the transition regimes of the gas–liquid flow in a two-dimensional bubble column applying various signal processing techniques for laser Doppler velocimetry. Brenn et al. (2002) studied both liquid and bubble velocities and the size distribution of the bubbles at different superficial gas velocities for small bubbles using a model bubble column and compared the results with results for larger bubbles obtained by other authors to check the accuracy of PDA. Munoz-Cobo et al. (2012) used Laser Doppler Anemometry to measure liquid velocity and turbulence intensity. The LDV techniques cannot be applied for homogeneous regime study of bubble column and difficulties in measurement are also found in cylindrical bubble columns when fractional gas holdup exceeds 10%.

2.6.5 Pressure Fluctuation:

Pressure fluctuation in the column was collected by the pressure transducers mounted on the column wall through plastic tubing. The current produced in the transducer due to the pressure signal was converted into voltage signal by passing through a resistor. The analog voltage was then converted to digital format with the help of an analog to digital converter. These data were then processed through a data

acquisition system and a personal computer to provide useful hydrodynamics details about the bubble column.

The Pressure Fluctuation technique can be used to determine the variation of axial gas holdup, bubble size and flow regime transition of bubble column [Tang and Heindel (2006)]. This technique is safe, simple, cheap and non-invasive. This technique can be applied to opaque fluid and vessels without the knowledge of fluid properties at high temperature and pressure [Tang and Heindel (2006)]. Flow structure determination using Pressure Fluctuation technique is not direct and requires data processing techniques such as statistical, spectral, fractal, time-domain, time–frequency and deterministic chaos analyses [Gourich et al. (2006); Vial et al. (2000)]. Statistical analysis does not give more information except transitions detection. Spectral analysis gives information of flow patterns, but impossible to find the transitions. Fractal analysis accurately indicates regimes, but on the contrary, is a time taking process. But the time-frequency analysis is most useful for non-stationary phenomena [Vial et al. (2000)].

2.6.6 Particle Image Velocimetry (PIV):

With the help of Wavelet transforms the shape, size and energy of individual bubble of a two-dimensional bubble column can be obtained from Particle Image Velocimetry data [Sathe et al. (2011)]. PIV technique can be used for the liquid flow map measurement [Luo and Al-Dahhan (2008)]. This technique gives real-time velocity maps by using CCD cameras along with computing hardware [Xiao et al. (2012)]. PIV has been used to measure gas holdups, interfacial areas and local bubble size distributions [Laakkonen et al. (2005a)], shear stress and filtration performance data[Yeo et al. (2007)]. PIV is a non-intrusive, advanced flow visualization technique

with high sensitivity that provides information about the whole flow field [Seeger et al. (2003), Xiao et al. (2013)]. However identification of bubbles is a time-consuming process as more number of bubbles are to be analysed to determine the average values [Benkrid et al. (2002)]. The images of the calibration target give the calibration constants for PIV technique [Sathe et al. (2011)].

In PIV measurements, the flow field is illuminated by a laser sheeting technique and the image of the flow field was taken by a high-resolution CCD camera at a high framing rate. These images are analysed using software. Presence of a large number of bubbles weakens the quality of the image. Wall effects on imaging can be avoided by placing the camera and the light source in opposite to each other. But due to blurriness in the images this arrangement is not suitable for large volume and high concentration of bubble. Hence, a laser light sheet is being illuminated perpendicular to the camera in order to minimize background noise [Laakkonen et al. (2005b)].

2.6.7 Tomography:

In a tomography process response from a system of sensors is analysed and a 3D image is reconstructed. Tomography is of two types (1) Hard-field tomography where the medium sensitivity is independent of the distribution of the measured parameters of the whole volume; and (2) Soft-field tomography in which the medium sensitivity is the function of the distribution of the measured parameters of the whole volume [Wahab et al. (2015)]. Depending upon the type of radiation used tomography is of different types.

2.6.7.1 X-Ray Computed Tomography (XRCT): It employs a scanning electron beam as radiation ray. The local mass density of the phases present along the transmitted path of the X-rays is calculated from attenuation measurements of the beam.

The three-dimensional density distributions of phases with high resolution are obtained from attenuation data of different beam paths from different orientations [Prasser et al. (2005)]. XRCT gives high spatial and temporal resolution [Zhang et al. (2013)]. The resolution to the center of the bed is not poor as in case of soft-field technique and the direction of a field line is not changed by the medium [Saayman et al. (2013)]. The XRT technique is not useful for visualizing bubbles at high operating velocities and shows artificial coalescence that requires more exploration [Saayman et al. (2013); Zhang et al. (2013)]. This technique is used to measure local time-averaged gas holdup, identification of the flow regimes (flooded, loaded, completely dispersed and gas recirculation) and bubble size distribution [Ford et al. (2008); Zhang et al. (2013)].

2.6.7.2 Optical Tomography (OT): In OT a beam of light (laser or LED) is transmitted through the bubble column. The electrical signal is used for image reconstruction using PC loaded with data acquisition algorithms [Ibrahim et al. (2012)]. This technique is applied to determine local bubble concentrations and bubble flow in a low gas fraction in vertical bubble columns and vertical pipelines.

2.6.7.3 Ultrasonic Computed Tomography(UCT): It is based on attenuation of the ultrasonic beam. It is a non-invasive measurement technique which can be used to investigate time-averaged holdup distributions of phases and their flow structure [Rahiman et al. (2014); Supardan et al. (2007)]. To get accurate results, UCT experiments are carried out at low gas velocity [Supardan et al. (2007)].

2.6.7.4 Gama Ray Computed Tomography (GRCT): In this technique Gama radiation from the source is transmitted through the medium and then collected by the detector placed on the opposite side of the column. It is used for visualization of phases and to provide information about the structure and composition of the phases in

multiphase systems. This technique can measure phase distributions very accurately, but it is a slow technique [Zhang et al. (2013)].

2.6.7.5 Electrical Resistance Tomography (ERT): Electrical Resistance Tomography provides colour coded images of phases based on the measurement of conductivity of continuous and dis-continuous phases [Razzak et al. (2009)]. By applying an AC current between two adjacent electrodes, corresponding voltage between other adjacent electrodes are measured and the same is repeated for all electrode pairs combinations to get a complete structure of data. These data are fed to a personal computer (PC) preloaded with a reconstruction algorithm to produce quantitative images. ERT is an advanced, non-invasive, fast imaging technique that can be used for online monitoring inside flow behaviour of bubble column in different axial and radial locations. This technique is suitable to provide real time data for small and large opaque systems with highly fluctuating flow. The advantage for the application of ERT is due to its low construction cost and high safety [Jin et al. (2007); Razzak et al. (2009); Jin et al. (2013); Babaei et al. (2014)]. However, the reconstruction image of ERT technique is of low optical resolution [Jin et al. (2007)]. It can be used to estimate gas holdup, bubble size, rise velocity and their distribution, for visualization of the concentration profiles, fluid dynamic characteristics in gas–liquid flow, to measure velocity distributions in bubble columns [Jin et al. (2007); Razzak et al. (2009); Jin et al. (2013); Babaei et al. (2014)].

2.6.7.6 Electrical Impedance Tomography (EIT): It is an extension of Electrical Resistance Tomography. It is a non-intrusive and non-invasive in-line method that provides accurate results without any contamination [Rimpilainen et al. (2010)]. EIT is used for the measurement of volume fractions of solid and gas in solid-liquid flows and gas-liquid flows [George et al. (2000)].

2.6.7.7 Electrical Capacitance Tomography: ECT is a non-intrusive, non-invasive, high speed imaging technique to study hydrodynamics of bubble column. The technique can withstand high pressure and high temperature without any radiation [Zhang et al. (2014)]. This technique has the advantage of low cost and real-time measurement ability [Asencio et al. (2015)].

2.6.7.8 Electrical Capacitance Volume Tomography: It is an extension of ECT tomography developed to provide direct 3-D imaging [Wang et al. (2014)]. It provides high temporal resolution but poor spatial resolution for which small objects cannot be analyzed [Chandrasekera et al. (2005)].

2.6.8 Radiography:

In this group of techniques attenuation of acoustic signal is being used for the hydrodynamic study of bubble column. The acoustic signals are either passed through the medium or generated due to the vibration of the medium. The acoustic signal may be in the range of ultrasound also.

The ultrasound can be used for particle sizing and to measure bubble velocities, interfacial areas, phase holdup measurements, their cross-sectional distributions and for the flow structure analysis [Stolojanu and Prakash (1997); Widyanto et al. (2006); Shukla and Prakash (2006)].

2.6.9 Acoustic Emission:

Acoustic technique is based on resonance frequency of the pulsating bubbles [Diaz et al.(2008)]. Therefore, it is not influenced by turbulence. Leighton and Walton (1987) also pointed out that surface waves are due to local liquid movements. Volume pulsations of bubbles influence liquid movements to a long distance.

The techniques for measurement of bubble size using a probe are capable of measuring local values of bubble size and number [Buchholz and Schügerl (1979)]. Vazquez et al. (2005) compared photographic and acoustic techniques with measurements using inverted funnel method and found that acoustic method is as accurate as optical method. It is not essential to use industrial hydrophones, but piezo-electric element can be used to get accurate estimates of bubble size. The processing of acoustic signal is faster than image analysis in case of photographic technique [Vazquez et al. (2005)]. The acoustic technique does provide no information about the bubble shape. Probe techniques, in general, do not provide total number of bubbles at a particular time. Optical probes works in a clear liquid, conductivity probes require sufficient ions in the solution. Acoustic technique does not have any such limitation. However, few shortcomings have to be addressed. Applications of acoustic techniques in chemical engineering processes have been reviewed by Boyd and Varley (2001).

Though, a hydrophone captures acoustic signal in the entire column, however, it requires the signal to be measured for some time so that thus obtained time-series can be converted to frequency domain. Local bubble size distribution measurement using this technique does not seem to be reported in literature.

Usry et al. (1987) measured acoustic signals and volumetric mass-transfer coefficient, $k_L a_i$, in an agitated tank and observed that both are inter-related though no quantitative relationship was proposed. However, it shows the possibility of using the acoustic signals to monitor the mass-transfer process.

Estimation of BSD from acoustic signals by different techniques was discussed by Al-Masery et al. (2005). Analysis of acoustic signals in the present work is based on the volume pulsation of bubbles. Strasberg (1956) used the following formula

developed by Minnaerf. It shows that the natural frequency of sound generated by simple volume pulsation, f_0, is inversely proportional to bubble radius, R.

$$f_0 = \left(3\gamma P_0 / \rho\right)^{1/2} / 2\pi R \tag{2.11}$$

where P_0 is the static pressure, $\gamma$is ratio of specific heats of gas in bubble and ρ is density of the liquid.

Al-Masery and Ali (2006) carried out a detailed study on bubble behaviour using acoustic technique. The effect of antifoam agents (5% and 10%) on hydrodynamics and bubble behaviour in bubble columns were studied for air-water system. In presence of antifoam chemicals average bubble diameter increased and gas holdup decreased. The BSD was homogeneous in absence of antifoam agents. For antifoam solutions it was heterogeneous. Improvement of the acoustic technique used to get estimates of the average bubble size and its distribution was felt [Al-Masery and Ali (2006)].

Based on the above discussion it was observed that development of acoustic method of measurement of bubble size and interfacial area is important from the point of view that the technique may be useful for opaque system either due to opaque wall or due to presence of impurities, suspended coloured particle or microbial flocks. The results will be useful for the design of bubble column or air-lift bioreactors. In the literature hydrophones were used but in the present it was decided to use inexpensive small condenser mikes to record acoustic signals. A small mike may measure local variation of bubble diameter and interfacial area. With the computational power available at the desktop, able to measure acoustic signals, use of acoustic sensor can provide a cost effective measurement technique.

If a small acoustic transducer, can measure only local signals, then axial variation of bubble size can increase our understanding of the bubble coalescence and bubble breakup phenomena. This aspect has not been explored.

It is worth to study relationship between the acoustic signal and mass-transfer rate which is not yet well understood.

2.7 Objective of the present work:

Thus it has been decided to choose acoustic technique to study the following aspects of bubble columns:-

(i) Development of acoustic technique for determination of bubble size distribution Newtonian and power law fluids.

(ii) Measurement of local bubble diameter and its variation along the vertical direction for Newtonian and power law fluids.

(iii) Measurement of local interfacial area and its variation along the vertical direction Newtonian and power law fluids.

(iv) Validation of results with visual observation using photographic technique.

(v) Measurement of gas-liquid volumetric mass-transfer coefficient.

(vi) Estimation of volumetric mass-transfer using experimentally determined interfacial area.

The next chapter describes the details of the experimental set-up, experimental procedures, fluid properties, procedure for analysis of the acoustic data.